Observing dark energy dynamics with supernova, microwave background, and galaxy clustering

Jun-Qing Xia,[1] Gong-Bo Zhao,[1] Bo Feng,[2] Hong Li,[1] and Xinmin Zhang[1]

[1]*Institute of High Energy Physics, Chinese Academy of Science, P.O. Box 918-4, Beijing 100049, People's Republic of China*

[2]*Research Center for the Early Universe (RESCEU), Graduate School of Science, The University of Tokyo, Tokyo 113-0033, Japan*

(Received 15 December 2005; published 20 March 2006)

Observing dark energy dynamics is the most important aspect of the current dark energy research. In this paper we perform a global analysis of the constraints on the property of dark energy from the current observations. We pay particular attention to the effects of dark energy perturbations. Using the data from SNIa (157 gold sample), WMAP, and SDSS we find that the best fitting dark energy model is given by the dynamical model with the equation of state crossing -1. Nevertheless the standard ΛCDM model is still a good fit to the current data and evidence for dynamics is currently not very strong. We also consider the constraints with the recent released SNIa data from Supernova Legacy Survey.

DOI: 10.1103/PhysRevD.73.063521 PACS numbers: 98.80.Es, 98.80.Cq

I. INTRODUCTION

In 1998 the analysis of the redshift-distance relation of type Ia supernova (SNIa) had established that our Universe is currently accelerating [1,2]. Recent observations of SNIa have confirmed the accelerating expansion at a high confidence level [3–5]. The nature of dark energy (DE), the mysterious power to drive the expansion, is among the biggest problems in modern physics and has been studied widely. A cosmological constant, the simplest candidate of DE where the equation of state (EOS) w remains -1, suffers from the well-known fine-tuning and coincidence problems [6,7]. Alternatively, dynamical dark energy models with the rolling scalar fields have been proposed, such as quintessence [8,9], the ghost field of phantom [10], and the model of k essence which has a noncanonical kinetic term [11,12].

Given that currently we know very little on the theoretical aspects of dark energy, the cosmological observations play a crucial role in our understanding of dark energy. The model of phantom has been proposed in history due to the mild preference for a constant EOS smaller than -1 by the observations [10]. Although in this scenario dark energy violates the weak energy condition and leads to the problem of quantum instabilities [13], it remains possible in the description of the nature of dark energy [14].

An intriguing aspect in the study of dark energy is that the recent SNIa observations from the HST/GOODS program [4], combined together with the previous supernova data, somewhat favor the dynamical dark energy model with an equation of state getting across -1 during the evolution of the Universe [15–18]. Although the conventional scalar dark energy models also show dynamical behaviors with redshift, due to the instabilities of perturbations they cannot preserve the required behavior of crossing the cosmological constant boundary [19–21]. The required model of dark energy has been called as quintom [18] in the sense that its behavior resembles the combined behavior of quintessence and phantom. However, the quintom models can be very different from the quintessence or phantom in the determination of the evolution and fate of the Universe [22]. There are a lot of interests in the literature recently in the building of quintomlike models. Minimally coupling to gravity, a simple realization of a quintom scenario is a model with the double fields of quintessence and phantom [18,23–28].[1] In such cases quintom would typically encounter the problem of quantum instability inherited from the phantom component. However, in the case of the single field scalar model of quintom, Ref. [34] added a high derivative term to the kinetic energy and its energy-momentum tensor is equivalent to the two-field quintom model. Such a model with a high derivative term is possibly without quantum instabilities, and as indicated by the SNIa observations, we are living with the ghosts [35].[2]

Observing the dark energy dynamics is currently the most important aspect of the dark energy study. Besides the SNIa data, a thorough investigation demands a fully consistent analysis of cosmic microwave background (CMB), large scale structure (LSS) with multiparameter freedoms. The aim of the current paper is to study the observational implications on dark energy in the consistent way, including the model of quintom. The previous fittings in the literature on quintomlike dark energy models have either fully or partially neglected the perturbations, which in some sense do not describe the realistic models with EOS across -1 and will lead to some bias in the fittings. In Ref. [20] we developed a self-consistent way to include the perturbations of quintom in light of the observations and studied it extensively on theoretical aspect. However, the fittings in Ref. [20] are preliminary and illustrative. In this paper we extend our previous work of Ref. [20] and study the full observational constraints on dynamical dark energy. In particular we pay great attention to the effects of dark energy perturbations when the equation of state gets

[1]Given some interactions between the dark energy sector with other sectors, the crossing behavior is viable; see e.g. [29–33].

[2]For another interesting single field quintom model building see [36].

across -1. Our paper is structured as follows: In Sec. II we describe the method and the data; in Sec. III we present our results on the determination of cosmological parameters with the first-year Wilkinson Microwave Anisotropy Probe (WMAP) [37], SNIa [4,38], and Sloan Digital Sky Survey (SDSS) [39] data by global fittings using the Markov chain Monte Carlo (MCMC) techniques [40–42]; finally we present our conclusions in Sec. IV.

II. METHOD AND DATA

In this section we first present the general formula of the dark energy perturbations in the full parameter space of w especially when it crosses over the cosmological constant boundary. Throughout, we assume a flat universe and our formula can be generalized to nonflat cases straightforwardly. In our MCMC fittings to WMAP, SNIa, and SDSS, we adopt a specific parametrization of the equation of state.

Despite our ignorance of the nature of dark energy, it is natural to consider the DE fluctuation whether DE is regarded as scalar field or fluid. In the extant cases like the two-field-quintom model as well as the single field case with a high derivative term [20], the perturbation of DE is shown to be continuous when the EOS gets across -1. For the conventional parameterized equation of state one can reconstruct easily the potential of the scalar dark energy if the EOS does not get across -1. Resembling the multifield model of quintom or that with high derivative terms, the potential of the quintom dark energy can be directly reconstructed from the parameterized EOS on either side of the cosmological constant boundary.[3] In this paper we give a self-consistent method to handle the perturbation in all the allowed range of EOS especially for the region where EOS evolves close to and crosses -1.

For the parametrization of the EOS which gets across -1, first we introduce a small positive constant ϵ to divide the full range of the allowed value of the EOS w into three parts: (1) $w > -1 + \epsilon$; (2) $-1 + \epsilon \geq w \geq -1 - \epsilon$; and (3) $w < -1 - \epsilon$. Working in the conformal Newtonian gauge, one can describe the perturbations of dark energy as follows [43]:

$$\dot{\delta} = -(1 + w)(\theta - 3\dot{\Phi}) - 3\mathcal{H}(c_s^2 - w)\delta, \qquad (1)$$

$$\dot{\theta} = -\mathcal{H}(1 - 3w)\theta - \frac{\dot{w}}{1 + w}\theta + k^2\left(\frac{c_s^2\delta}{1 + w} + \Psi\right). \qquad (2)$$

[3]Although the multifield dark energy models are more challenging on theoretical aspects of naturalness, given that we know very little on the nature of dark energy, the energy momentum of such models can be identified with single field scalar dark energy with high derivative kinetic terms [34]. Our phenomenological formula of perturbations on DE corresponds to such models of multifield (quintom) with a negligible difference around the crossing point of -1 [20].

Neglecting the entropy perturbation contributions, for the regions (1) and (3) the EOS is always greater than -1 and less than -1, respectively, and perturbation is well defined by solving Eqs. (1) and (2). For the case (2), the perturbation of energy density δ and divergence of velocity, θ, and the derivatives of δ and θ are finite and continuous for the realistic quintom dark energy models. However for the perturbations of the parametrized quintom there is clearly a divergence. In our study for such a regime, we match the perturbation in region (2) to the regions (1) and (3) at the boundary and set [20]

$$\dot{\delta} = 0, \qquad \dot{\theta} = 0. \qquad (3)$$

In our numerical calculations we have limited the range to be $|\Delta w = \epsilon| < 10^{-5}$ and we find our method is a very good approximation to the multifield quintom, with the accuracy being greater than 99.999%. For more details of this method we refer the readers to our previous companion paper [20].

In the study of this paper the parameterized EOS of dark energy is taken by [44]

$$w(z) = w_0 + w_1\frac{z}{1 + z}. \qquad (4)$$

The method we adopt is based on the publicly available Markov chain Monte Carlo package COSMOMC [45,46], which has been modified to allow for the inclusion of dark energy perturbations with EOS getting across -1 [20]. We sample the following eight-dimensional set of cosmological parameters:

$$\mathbf{p} \equiv (\omega_b, \omega_c, \Theta_S, \tau, w_0, w_1, n_s, \log[10^{10}A_s]), \qquad (5)$$

where $\omega_b = \Omega_b h^2$ and $\omega_c = \Omega_c h^2$ are the physical baryon and cold dark matter densities relative to critical density, Θ_S is the ratio (multiplied by 100) of the sound horizon and angular diameter distance, τ is the optical depth, A_s is defined as the amplitude of initial power spectrum, and n_s measures the spectral index. Basing on the Bayesian analysis, we vary the above eight parameters fitting to the observational data with the MCMC method. We take the weak priors as $\tau < 0.8$, $0.5 < n_s < 1.5$, $-3 < w_0 < 3$, $-5 < w_1 < 5$, a cosmic age top hat prior as $10\,\mathrm{Gyr} < t_0 < 20\,\mathrm{Gyr}$. The choice of priors on w_0, w_1 have been set to allow for spread in both of the parameters simultaneously. Furthermore, we make use of the Hubble space telescope measurement of the Hubble parameter $H_0 = 100h\ \mathrm{km\,s^{-1}\,Mpc^{-1}}$ [47] by multiplying the likelihood by a Gaussian likelihood function centered around $h = 0.72$ and with a standard deviation $\sigma = 0.08$. We impose a weak Gaussian prior on the baryon and density $\Omega_b h^2 = 0.022 \pm 0.002$ (1σ) from big bang nucleosynthesis [48].

In our calculations we have taken the total likelihood to be the products of the separate likelihoods of CMB, SNIa, and LSS. Alternatively defining $\chi^2 = -2\log\mathcal{L}$, we get

$$\chi^2_{\mathrm{total}} = \chi^2_{\mathrm{CMB}} + \chi^2_{\mathrm{SNIa}} + \chi^2_{\mathrm{LSS}}. \qquad (6)$$

In the computation of CMB we have included the first-year temperature and polarization data [37,49] with the routine for computing the likelihood supplied by the WMAP team [50]. In the computation of nonlinear evolution of the matter power spectra we have used the code of HALOFIT [51] and fitted to the 3D power spectrum of galaxies from the SDSS [39] using the code developed in Ref. [52]. In the calculation of the likelihood from SNIa we have marginalized over the nuisance parameter [53]. For the main results of the current paper the supernova data we use are the ''gold'' set of 157 SNIa published by Riess *et al.* in [4]. In addition, we also consider the constraints from the distance measurements of the 71 high redshift type Ia supernova discovered during the first year of the five-year Supernova Legacy Survey (SNLS) [38].

For each regular calculation, we run six independent chains comprising of 150 000–300 000 chain elements and spend thousands of CPU hours to calculate on a cluster. The average acceptance rate is about 40%. We test the convergence of the chains by Gelman and Rubin criteria and find $R - 1$ is of order 0.01 which is more conservative than the recommended value $R - 1 < 0.1$.

III. RESULTS

In this section we present our results, particularly focusing on the effects of the dark energy perturbation. We start with the descriptions on the background parameters, then present the constraints on dark energy parameters. At last we give our constraints on dark energy from the recent observational data of SNLS.

In Table I we list the mean 1σ constraints on the parameters with and (incorrectly) without DE perturbations. We find that almost all the cosmological parameters are well determined in both cases. However, the reionization depth seems to be an exception where a vanishing τ cannot be ruled out. We notice the determination on τ is prior dependent. For example the WMAP Collaboration has taken a prior like $\tau < 0.3$ [50,54,55], which leads to a relatively stringent constraint on τ by the observations and a nonzero τ is particularly favored by the high power of temperature-polarization cross correlation on the largest scales [56]. However, when the strong prior on τ is dropped, one will in general get a less stringent bound from the full observational constraints, as also shown in Ref. [52]. The prior on τ is somewhat crucial for our parameter estimation since its effects on CMB can be compensated with the tilt of the primordial scalar as well as the tensor spectrum. As we will show below it also will be correlated with the dark energy parameters due to the integrated Sachs-Wolfe (ISW) effects.

In Fig. 1 also we delineate the corresponding posterior one dimensional marginalized distributions of the cosmological parameters from the combined observations of WMAP, SDSS, and SNIa. The dotted vertical lines show the quantity of every parameter with and (incorrectly) without DE perturbation giving the maximum likelihood. Because of the fact that the peaks in the likelihood are different from the corresponding expectation values, the dashed lines in Fig. 1 do not lie at the center of the projected likelihoods. A vanishing τ cannot be excluded by the full combined observations at high confidence level.

TABLE I. Mean 1σ constraints on cosmological parameters using different combination of WMAP, SNIa, and SDSS information with/without DE perturbation. For the weakly constrained parameters we quote the 95% upper limit instead.

	With DE perturbation			(Incorrectly) without DE perturbation		
	WMAP	WMAP + SN	WMAP + SN + SDSS	WMAP	WMAP + SN	WMAP + SN + SDSS
$\Omega_b h^2$	$0.0232^{+0.0010}_{-0.0011}$	$0.0234^{+0.0010}_{-0.0011}$	0.0232 ± 0.0010	0.0235 ± 0.0013	0.0232 ± 0.0011	0.0230 ± 0.0009
$\Omega_c h^2$	0.124 ± 0.016	0.128 ± 0.018	0.123 ± 0.010	0.111 ± 0.020	0.119 ± 0.018	0.122 ± 0.010
Θ_S	1.046 ± 0.006	1.047 ± 0.006	1.046 ± 0.005	1.046 ± 0.006	1.046 ± 0.006	1.046 ± 0.005
τ	$<0.256(95\%)$	$<0.264(95\%)$	$<0.256(95\%)$	$<0.399(95\%)$	$<0.324(95\%)$	$<0.246(95\%)$
w_0	$-0.732^{+0.623}_{-0.613}$	$-1.172^{+0.231}_{-0.226}$	$-1.167^{+0.191}_{-0.190}$	$-0.617^{+0.193}_{-0.190}$	$-1.080^{+0.105}_{-0.087}$	$-1.098^{+0.078}_{-0.080}$
w_1	$<1.59(95\%)$	$0.361^{+0.842}_{-0.883}$	$0.597^{+0.657}_{-0.713}$	$<0.832(95\%)$	$0.359^{+0.287}_{-0.179}$	$0.416^{+0.293}_{-0.153}$
n_s	$0.977^{+0.029}_{-0.030}$	$0.986^{+0.030}_{-0.031}$	0.982 ± 0.030	$0.995^{+0.045}_{-0.041}$	$0.981^{+0.032}_{-0.033}$	$0.970^{+0.024}_{-0.025}$
$\log[10^{10}A_s]$	3.181 ± 0.134	3.207 ± 0.132	$3.180^{+0.125}_{-0.123}$	$3.245^{+0.202}_{-0.183}$	$3.206^{+0.153}_{-0.150}$	$3.157^{+0.118}_{-0.119}$
Ω_Λ	$0.703^{+0.073}_{-0.072}$	0.678 ± 0.045	$0.681^{+0.031}_{-0.030}$	0.681 ± 0.086	0.697 ± 0.048	0.686 ± 0.031
Age/Gyr	13.45 ± 0.27	$13.57^{+0.30}_{-0.29}$	13.67 ± 0.24	13.60 ± 0.30	13.62 ± 0.29	13.67 ± 0.23
Ω_m	$0.297^{+0.072}_{-0.073}$	0.322 ± 0.045	$0.319^{+0.030}_{-0.031}$	0.319 ± 0.086	0.303 ± 0.048	0.314 ± 0.031
σ_8	$0.927^{+0.152}_{-0.154}$	$0.913^{+0.148}_{-0.150}$	$0.854^{+0.096}_{-0.097}$	0.818 ± 0.120	$0.890^{+0.117}_{-0.118}$	$0.882^{+0.073}_{-0.072}$
z_{re}	$14.35^{+4.71}_{-4.68}$	$14.72^{+4.90}_{-4.77}$	$14.41^{+4.97}_{-4.83}$	$17.17^{+6.94}_{-6.27}$	$15.49^{+5.69}_{-5.38}$	$13.73^{+4.78}_{-4.72}$
H_0	$71.71^{+7.95}_{-8.02}$	$68.66^{+2.44}_{-2.45}$	$67.90^{+2.48}_{-2.46}$	$66.04^{+6.41}_{-6.47}$	$68.89^{+2.52}_{-2.61}$	$68.07^{+2.35}_{-2.33}$
χ^2/d.o.f.	1429.1/1342	1610.4/1499	1633.2/1518	1428.4/1342	1610.6/1499	1634.1/1518

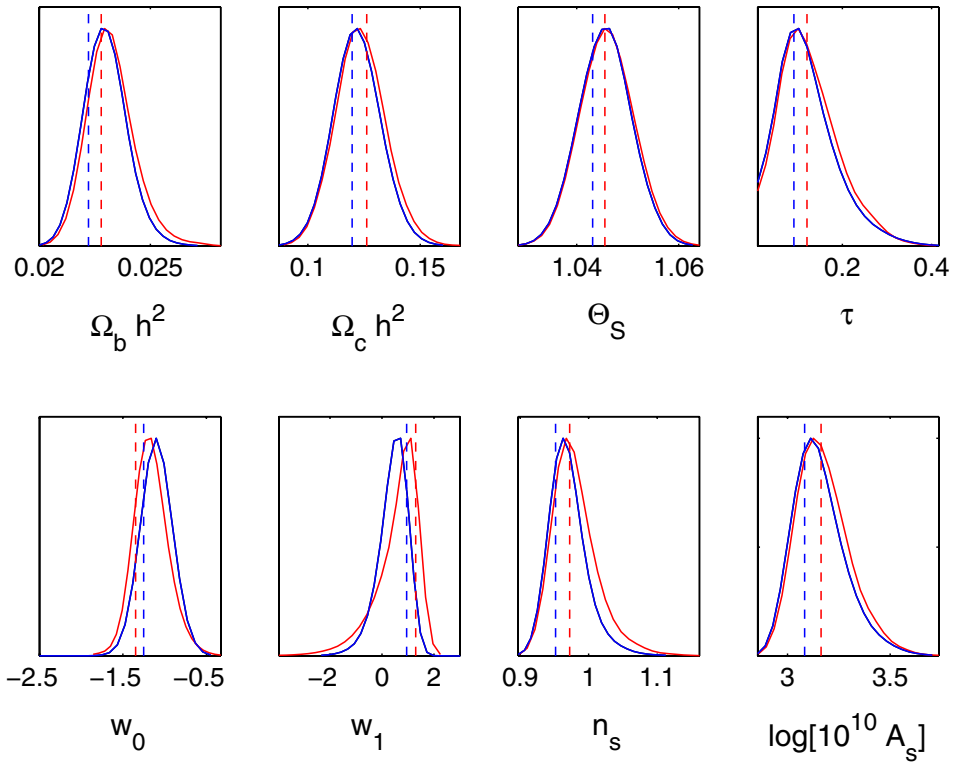

FIG. 1 (color online). 1-D constraints on individual parameters using WMAP + 157 gold SNIa + SDSS with our eight-parameter parametrization discussed in the text. Solid curves illustrate the marginalized distribution of each parameter with and (incorrectly) without DE perturbation. Dotted vertical lines shows the quantity of every parameter with and (incorrectly) without DE perturbation giving the maximum likelihood.

For the order of parameters listed in (5) the best fit values constrained by the full data set (WMAP + SNIa + SDSS) is $\mathbf{p} = (0.023, 0.12, 1.04, 0.16, -1.30, 1.25, 0.995, 3.23)$. And for comparison the resulting parameters when switching off dark energy perturbations are given by $\mathbf{p} = (0.023, 0.12, 1.05, 0.14, -1.15, 0.63, 0.962, 3.14)$.

Comparing with the bottom of Table I, although the minimum χ^2 values have not been affected significantly (up to 1) by dark energy perturbations, all the best fit parameters have been changed. Moreover, the allowed parameter space has been changed a lot and the constraints on the background parameters have been less stringent when including the dark energy perturbations. This also can be clearly seen from the two-dimensional contour plots on the background parameters in Fig. 2. The reason is not difficult to explain. The ISW effects of the dynamical dark energy boosts the large scale power spectrum of CMB [20]. For a constant equation of state Ref. [57] has shown that when the perturbations of dark energy have been neglected incorrectly [58], a suppressed ISW will be resulted for quintessencelike dark energy and on the contrary, an enhanced ISW is led to by phantomlike dark energy. In this sense if we neglect dark energy contributions, there will be less degeneracy in the determination of dark energy as well as the relative cosmological parameters. However, dark energy perturbations are anticorrelated with the source of matter perturbations and this will lead to a compensation on the ISW effects, which result in a large parameter degeneracy [57]. In fact, as we have shown, crossing over the cosmological constant boundary would not lead to distinctive effects [20], hence the effects of our smooth parametrization of EOS on CMB also can be somewhat identified with a constant effective equation of state [59]

$$w_{\text{eff}} \equiv \frac{\int da \Omega(a) w(a)}{\int da \Omega(a)}; \tag{7}$$

however, the SNIa and LSS observations will break such a degeneracy. Thus for the realistic cases of including dark energy perturbations, the correlations between the dark energy and the background parameters as well as the auto correlations of the background cosmological parameters have been enlarged, as can be seen from Fig. 2.

The contribution of dark energy perturbation affects significantly the distribution of w_0 and w_1, which also can be seen from Fig. 3 on the constrains in the (w_0, w_1) plane. For the parameters (w_0, w_1) the inclusion of the dark energy perturbation change its best fit values from $(-1.15, 0.63)$ to $(-1.30, 1.25)$. In Fig. 3, from outside in, the contours shrink with adding 157 SNIa data provided by Riess *et al* and SDSS information. Dark energy perturba-

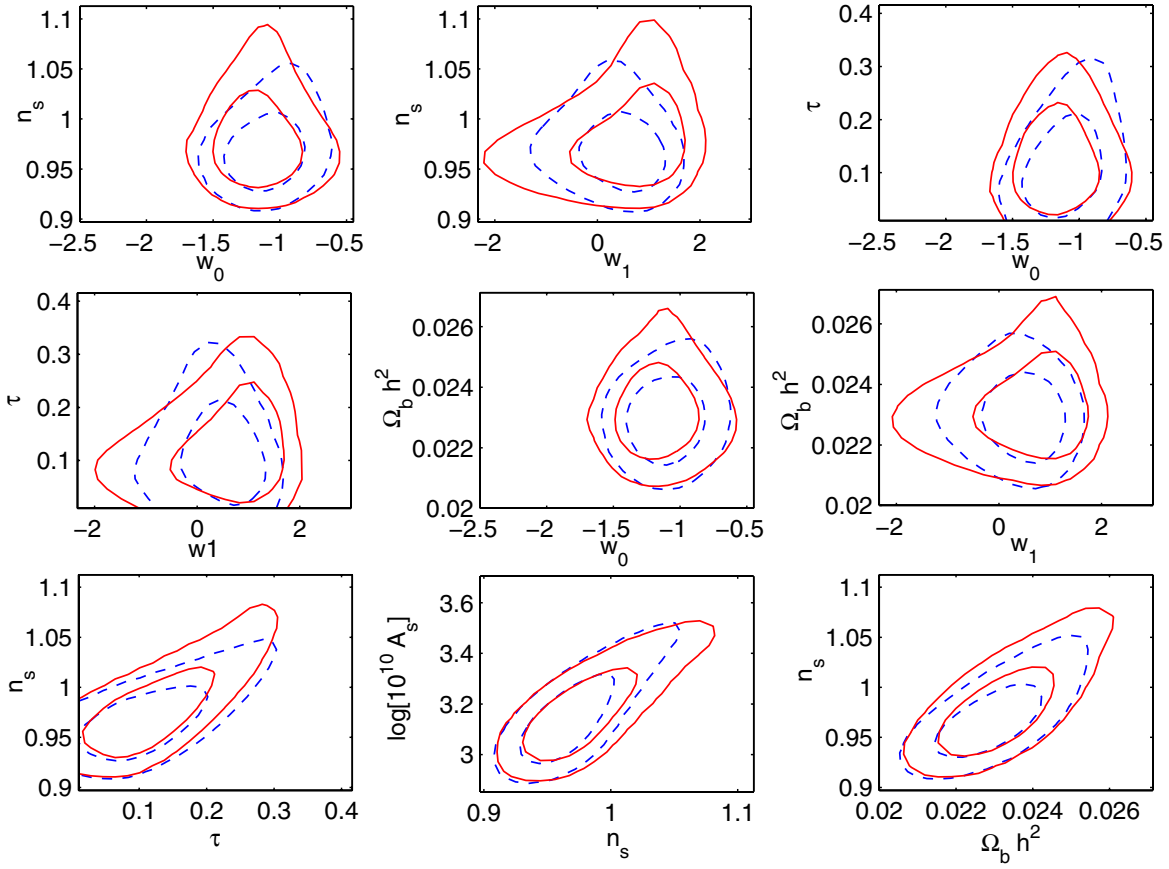

FIG. 2 (color online). Sampled 2-D contours of the background parameters and also the contours among dark energy and the background parameters. Here we use the same parametrization and data sets as FIG. 2, solid and dashed lines are for perturbated and unperturbated DE, respectively.

tion introduces more degeneracy between w_0 and w_1 thus enlarges the contours significantly. For the discussion on dynamical dark energy we have separated the space of $w_0 - w_1$ into four areas by the lines of $w_0 = -1$ and $w_0 + w_1 = -1$. The areas will then represent the quintessence where the EOS is always no less than -1 (the area with

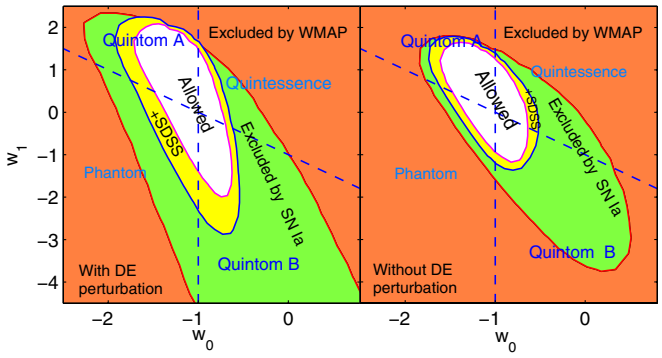

FIG. 3 (color online). 95% constraints in the (w_0, w_1) plane with and (incorrectly) without dark energy perturbation from left to right. Shaded dark region is excluded by WMAP only for our eight-parameter estimation. The dashed lines stand for $w_0 = -1$ and $w_0 + w_1 = -1$; see the text for details.

$w > 1$ can be reached by quintessence with a negative potential [60]), Quintom A where w is phantomlike today but quintessencelike in the past, phantom where the EOS is always no larger than -1, and Quintom B where dark energy has $w > -1$ today but $w < -1$ at higher redshifts. From the figure we can see that dynamical dark energy with the four types are all allowed by the current observations, and Quintom A seems to cover the largest area in the two-dimensional contours with all the data we used.

As shown in Fig. 3, w_0 and w_1 are in strong correlations. The constraints on $w(z)$ are perhaps relatively model independent, as suggested by Ref. [61]. Following [62] we obtain the constraints on $w(z)$ by computing the median and 1, 2σ intervals at any redshift. In Fig. 4 we plot the behavior of the dark energy EOS as a function of redshift z; we find that at redshift $z = 0.3$ the constraint on the EOS is relatively the most stringent. One can see that the perturbation reinforces the trend of DE to cross -1 at $z \sim 0.3$. However, due to the limitation of the observational data, the quintom scenario is only favored at 1σ by the full data set of WMAP, SDSS, and SNIa. We find the value at $z = 0.3$ is restricted at

$$w(z = 0.3) = -1.002^{+0.044+0.180}_{-0.079-0.159} \quad (8)$$

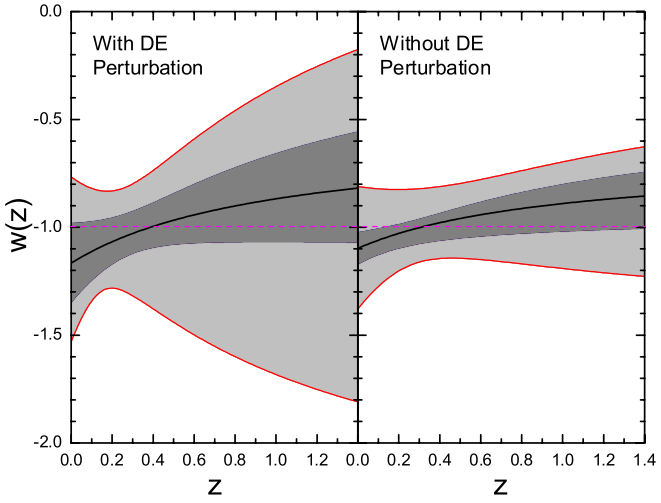

FIG. 4 (color online). Constraints on $w(z)$ using WMAP + 157 gold SNIa data + SDSS with/without DE perturbation. Median (central line), 68% (inner, dark shaded area) and 95% (outer, light shaded area) intervals of $w(z)$ using two-parameter expansion of the EOS in (4).

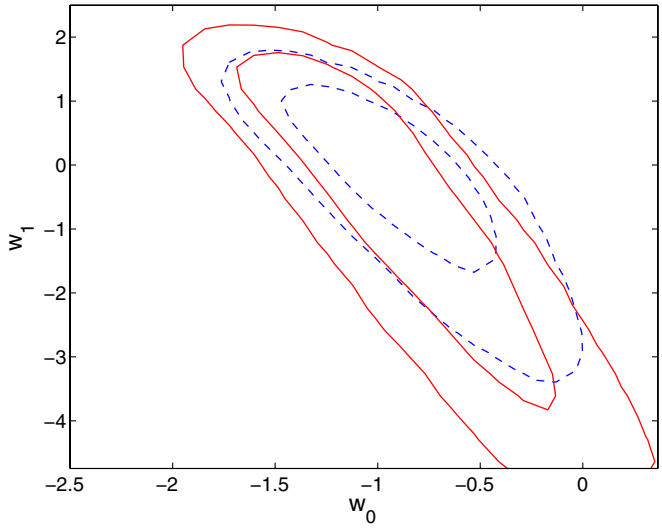

FIG. 5 (color online). Two-dimensional constraints on the parameters of dynamical dark energy from the combined constraints of SNLS, WMAP, and SDSS. The solid and dotted lines are the constraints with and (incorrectly) without dark energy perturbations, respectively.

for the case without dark energy perturbations and

$$w(z = 0.3) = -1.029^{+0.108+0.230}_{-0.098-0.288} \tag{9}$$

when including dark energy perturbations. Correspondingly at redshift $z = 1$ the constraints turn out to be

$$w(z = 1) = -0.890^{+0.180+0.193}_{-0.159-0.301} \tag{10}$$

without perturbations and

$$w(z = 1) = -0.868^{+0.215+0.520}_{-0.204-0.815} \tag{11}$$

when including dark energy perturbations. One should bear in mind that such a constraint is not really model independent, as shown in Refs. [63,64].

Recently the authors of Ref. [38] made the distance measurements to 71 high redshift type Ia supernovae discovered during the first year of the five-year Supernova Legacy Survey. SNLS will hopefully discover around 700 type Ia supernovae, which is an intriguing ongoing project. Following Ref. [38] we combine the ''new 71 high redshift SNIa data $\bigoplus$ the 44 nearby SNIa,'' together with WMAP and SDSS. We plot the constraints on the dark energy parameters in Fig. 5. We find the current data of SNLS are very weak in the determination of dark energy parameters. Although our best fit values are given with a quintomlike dark energy, $(w_0, w_1) = (-1.47, 1.44)$, a cosmological constant fits well with SNLS in the 1σ region.[4]

[4]Reference [65] made some study on SNLS implications of dynamical dark energy using SNIa data only.

IV. DISCUSSION AND CONCLUSION

In this paper we have performed an analysis of global fitting on the EOS of dark energy from the current data of SNIa, WMAP, and SDSS. Dark energy perturbation leaves imprints on CMB through ISW effects and changes the matter power spectrum by modifying the linear growth factor as well as the transfer function. Our results show that when we include the perturbations of dark energy, the current observations allow for a large variation in the EOS of dark energy with respect to redshift.[5] A dynamical dark energy with the EOS getting across -1 is favored at 1σ with the combined constraints from WMAP, SDSS, and the gold data set of SNIa by Riess *et al.* When we use the recently released SNLS data and the nearby data of type Ia supernova instead, the parameter space is enlarged and a cosmological constant is well within 1σ, although a quintom dynamical dark energy is still mildly favored.

In our all results, the perturbation of dark energy plays a significant role in the determination of cosmological parameters. Neglecting the contributions of dark energy perturbation will lead to biased results which are more stringent than the real cases. In the next decade, there will be many ongoing projects in the precise determination of cosmological parameters. We can hopefully detect the signatures of dynamical dark energy like quintom through

[5]Reference [66] studied the perturbations of dynamical dark energy only for the regime where $w > -1$ and Ref. [67] considered both the cases for $w > -1$ and $w < -1$ but did not include the perturbations for quintomlike dark energy; previous global analysis like Refs. [61,68] did not consider dark energy perturbations.

global fittings to the observations, where it is crucial for us to include the contributions of dark energy perturbations.

ACKNOWLEDGMENTS

Our MCMC chains were finished in the Shuguang 4000A system of the Shanghai Supercomputer Center (SSC). This work is supported in part by the National Natural Science Foundation of China under Grants No. 90303004, No. 10533010, and No. 19925523 and by the Ministry of Science and Technology of China under Grant No. NKBRSF G19990754. We thank Mingzhe Li for helpful discussions and Hiranya Peiris for comments on the manuscript.

[1] A. G. Riess *et al.* (Supernova Search Team Collaboration), Astron. J. **116**, 1009 (1998).
[2] S. Perlmutter *et al.* (Supernova Cosmology Project Collaboration), Astrophys. J. **517**, 565 (1999).
[3] J. L. Tonry *et al.* (Supernova Search Team Collaboration), Astrophys. J. **594**, 1 (2003).
[4] A. G. Riess *et al.* (Supernova Search Team Collaboration), Astrophys. J. **607**, 665 (2004).
[5] A. Clocchiatti *et al.* (the High Z SN Search Collaboration), astro-ph/0510155.
[6] S. Weinberg, Rev. Mod. Phys. **61**, 1 (1989).
[7] I. Zlatev, L.-M. Wang, and P. J. Steinhardt, Phys. Rev. Lett. **82**, 896 (1999).
[8] B. Ratra and P. J. E. Peebles, Phys. Rev. D **37**, 3406 (1988); P. J. E. Peebles and B. Ratra, Astrophys. J. **325**, L17 (1988).
[9] C. Wetterich, Nucl. Phys. **B302**, 668 (1988); C. Wetterich, Astron. Astrophys. **301**, 321 (1995).
[10] R. R. Caldwell, Phys. Lett. B **545**, 23 (2002).
[11] T. Chiba, T. Okabe, and M. Yamaguchi, Phys. Rev. D **62**, 023511 (2000).
[12] C. Armendariz-Picon, V. Mukhanov, and P. J. Steinhardt, Phys. Rev. Lett. **85**, 4438 (2000); Phys. Rev. D **63**, 103510 (2001).
[13] S. M. Carroll, M. Hoffman, and M. Trodden, Phys. Rev. D **68**, 023509 (2003); J. M. Cline, S.-Y. Jeon, and G. D. Moore, Phys. Rev. D **70**, 043543 (2004).
[14] See e.g. P. H. Frampton, Phys. Lett. B **555**, 139 (2003); V. Sahni and Y. Shtanov, J. Cosmol. Astropart. Phys. 11 (2003) 014; B. McInnes, J. High Energy Phys. 08 (2002) 029; V. K. Onemli and R. P. Woodard, Classical Quantum Gravity **19**, 4607 (2002); Phys. Rev. D **70**, 107301 (2004); I. Y. Aref'eva, A. S. Koshelev, and S. Y. Vernov, astro-ph/0412619; I. Y. Aref'eva and L. V. Joukovskaya, J. High Energy Phys. 10 (2005) 087.
[15] S. Nesseris and L. Perivolaropoulos, Phys. Rev. D **70**, 043531 (2004).
[16] U. Alam, V. Sahni, and A. A. Starobinsky, J. Cosmol. Astropart. Phys. 06 (2004) 008.
[17] D. Huterer and A. Cooray, Phys. Rev. D **71**, 023506 (2005).
[18] B. Feng, X. Wang, and X. Zhang, Phys. Lett. B **607**, 35 (2005).
[19] A. Vikman, Phys. Rev. D **71**, 023515 (2005).
[20] G. B. Zhao, J. Q. Xia, M. Li, B. Feng, and X. Zhang, Phys. Rev. D **72** 123515 (2005).
[21] L. R. Abramo and N. Pinto-Neto, astro-ph/0511562.
[22] B. Feng, M. Li, Y. S. Piao, and X. Zhang, Phys. Lett. B **634**, 101 (2006).
[23] Z.-K. Guo, Y.-S. Piao, X. Zhang, and Y.-Z. Zhang, Phys. Lett. B **608**, 177 (2005).
[24] W. Hu, Phys. Rev. D **71**, 047301 (2005).
[25] X. Zhang, hep-ph/0410292.
[26] R. R. Caldwell and M. Doran, Phys. Rev. D **72**, 043527 (2005).
[27] X.-F. Zhang, H. Li, Y.-S. Piao, and X. Zhang, Mod. Phys. Lett. A **21**,231 (2006).
[28] For an interesting variation see H. Wei, R. G. Cai, and D. F. Zeng, Classical Quantum Gravity **22**, 3189 (2005).
[29] G. Huey and B. D. Wandelt, astro-ph/0407196.
[30] X. J. Bi, B. Feng, H. Li, and X. M. Zhang, Phys. Rev. D **72**, 123523 (2005).
[31] H. Li, B. Feng, J. Q. Xia, and X. Zhang, astro-ph/0509272.
[32] S. Das, P. S. Corasaniti, and J. Khoury, astro-ph/0510628.
[33] B. Wang, Y. Gong, and E. Abdalla, Phys. Lett. B **624**, 141 (2005).
[34] M. Li, B. Feng, and X. Zhang, J. Cosmol. Astropart. Phys. 12 (2005) 002.
[35] S. W. Hawking and T. Hertog, Phys. Rev. D **65**, 103515 (2002).
[36] C. G. Huang and H. Y. Guo, astro-ph/0508171.
[37] C. L. Bennett *et al.* (WMAP Collaboration), Astrophys. J. Suppl. Ser..**148**, 1 (2003).
[38] P. Astier *et al.*, astro-ph/0510447.
[39] M. Tegmark *et al.* (SDSS Collaboration), Astrophys. J. **606**, 702 (2004).
[40] D. Gamerman, *Markov Chain Monte Carlo: Stochastic Simulation for Bayesian Inference* (Chapman and Hall, London, 1997).
[41] D. J. C. MacKay (2002), http://www.inference.phy.cam.ac.uk/mackay/itprnn/book.html.
[42] R. M. Neil (1993), ftp://ftp.cs.utoronto.ca/pub/radford/review.ps.Z.
[43] C. -P. Ma and E. Berschinger, Astrophys. J. **455**, 7 (1995).
[44] M. Chevallier and D. Polarski, Int. J. Mod. Phys. D **10**, 213 (2001); E. V. Linder, Phys. Rev. Lett. **90**, 091301 (2003).
[45] A. Lewis and S. Bridle, Phys. Rev. D **66**, 103511 (2002).
[46] Available from http://cosmologist.info.
[47] W. L. Freedman *et al.*, Astrophys. J. **553**, 47 (2001).
[48] S. Burles, K. M. Nollett, and M. S. Turner, Astrophys. J. **552**, L1 (2001).
[49] G. Hinshaw *et al.*, Astrophys. J. Suppl. Ser. **148**, 135 (2003).

[50] L. Verde *et al.* (WMAP Collaboration), Astrophys. J. Suppl. Ser. **148**, 195 (2003).
[51] R. E. Smith *et al.*, Mon. Not. R. Astron. Soc. **341**, 1311 (2003).
[52] M. Tegmark *et al.* (SDSS Collaboration), Phys. Rev. D **69**, 103501 (2004).
[53] For details see e.g. E. Di Pietro and J. F. Claeskens, Mon. Not. R. Astron. Soc. **341**, 1299 (2003).
[54] D. N. Spergel *et al.* (WMAP Collaboration), Astrophys. J. Suppl. Ser. **148**, 175 (2003).
[55] H. V. Peiris *et al.* (WMAP Collaboration), Astrophys. J. Suppl. Ser. **148**, 213 (2003).
[56] A. Kogut *et al.* (WMAP Collaboration), Astrophys. J. Suppl. Ser. **148**, 161 (2003).
[57] J. Weller and A. M. Lewis, Mon. Not. R. Astron. Soc. **346**, 987 (2003).
[58] For studies on dark energy perturbations see also R. Bean and O. Dore, Phys. Rev. D **69**, 083503 (2004); G. Huey, astro-ph/0411102.
[59] See e.g. L. M. Wang, R. R. Caldwell, J. P. Ostriker, and P. J. Steinhardt, Astrophys. J. **530**, 17 (2000).
[60] See e.g. G. N. Felder, A. V. Frolov, L. Kofman, and A. V. Linde, Phys. Rev. D **66**, 023507 (2002).
[61] U. Seljak *et al.*, Phys. Rev. D **71**, 103515 (2005).
[62] D. Huterer and M. S. Turner, Phys. Rev. D **64**, 123527 (2001).
[63] B. A. Bassett, P. S. Corasaniti, and M. Kunz, Astrophys. J. **617**, L1 (2004).
[64] J.-Q. Xia, B. Feng, and X. Zhang, Mod. Phys. Lett. A **20**, 2409 (2005).
[65] S. Nesseris and L. Perivolaropoulos, Phys. Rev. D **72**, 123519 (2005).
[66] Ch. Yeche, A. Ealet, A. Refregier, C. Tao, A. Tilquin, J.-M. Virey, and D. Yvon, astro-ph/0507170.
[67] P. S. Corasaniti, M. Kunz, D. Parkinson, E. J. Copeland, and B. A. Bassett, Phys. Rev. D **70**, 083006 (2004).
[68] S. Hannestad and E. Mortsell, J. Cosmol. Astropart. Phys. 09 (2004) 001; A. Upadhye, M. Ishak, and P. J. Steinhardt, Phys. Rev. D **72**, 063501 (2005).